Infrared Spectral Studies on Coordination Structure and Oxidation−Degradation for Cobalt(II) Salts of Ethylene−Methacrylic Acid Copolymer and Their Complexes with an Organic Amine

Shoichi Kutsumizu,*,† Hisako Kimura,† Fumihiko Mohri,† Hisaaki Hara,‡ Hitoshi Tachino,‡ Eisaku Hirasawa,‡ and Shinichi Yano†

Department of Chemistry, Faculty of Engineering, Gifu University, Yanagido 1-1, Gifu 501-11, Japan, and Technical Center, Du Pont-Mitsui Polychemicals Company, Ltd., Chigusa-kaigan 6, Ichihara, Chiba 299-01, Japan

Received April 11, 1995; Revised Manuscript Received December 4, 1995[⊗]

ABSTRACT: Coordination structure and oxidation−degradation were investigated for two types of ionomers, ethylene−methacrylic acid (5.4 mol %) copolymer partially neutralized with Co(II) and its complex salt with 1,3-bis(aminomethyl)cyclohexane [1,3-$(H_2NCH_2)_2C_6H_{10}$] (BAC), by using infrared (IR) spectroscopy and gas chromatography−mass spectrometry (GC−MS). The IR spectrum for the Co(II) salt was reversible with temperature when the sample was sealed from air with KBr windows, but irreversible in air, showing the presence of oxidation−degradation. The decomposition products were identified to be mainly alcohol, ketone, and alkanecarboxylic acid derivatives by the use of GC−MS spectrometry. The Co(II) complex salt with BAC, on the other hand, showed a reversible temperature dependence of the IR spectra, even when the sample was heated in air above the melting point of poly(ethylene) crystallites (∼90 °C). The difference in thermal stability between the two types of ionomers was well explained by the coordination structures of Co(II) ions. Finally, the present study demonstrated that the asymmetric COO^- stretching band for both ionomers significantly changes around a transition temperature (∼50 °C) of ionic aggregate regions, which gives evidence for an order−disorder transition model of ionic aggregate regions proposed by us.

Introduction

Ionomers are polymeric materials having a small number of ionic side groups in the hydrophobic backbone chains. The hydrophilic ionic groups are frequently separated from the hydrophobic polymer matrix to form ionic aggregates, such as multiplets or ionic clusters.[1] The formation of ionic aggregates usually provides a profound influence on physical properties such as bending modulus, tensile strength, impact resistance, and melt viscosity.[2−5] Therefore, it is very important to clarify the formation and structure of ionic aggregates. To date, various physical measurements have been carried out for several types of ionomers and many morphological models for the ionic clusters have been proposed,[1,6−9] but a convincing model has not yet been obtained because the ionic aggregates are on a nanometer scale.

In ethylene ionomers, we proposed a structural model[10−12] for ionic aggregates, and its revised version recently appeared:[13,14] The inside of ionic aggregates is an ordered assembly consisting of ionic groups and a small portion of backbone chains at room temperature, but when the temperature is increased, disorder occurs at a temperature (T_i) near 50 °C. When the sample is cooled from a temperature above T_i to room temperature, the disordered ionic aggregates very slowly transform into the ordered ionic aggregates, with a long relaxation time of about 40 days. We have demonstrated that the order−disorder transition model qualitatively explains most physical properties,[10−26] but the model has not been universally recognized since direct evidence is not obtained. Moreover, a few other models have been proposed for the change at T_i, for example, one relates the change at T_i to the melting of quasi-crystallites formed during annealing and another to the evaporation of residual water in the ionomers.

Infrared (IR) spectroscopy is a useful technique to investigate some local environments of ionic groups in ionomers.[27] To date, the coordination structure of ionic groups has been studied for ethylene ionomers,[28−36] and it has been pointed out that the coordination structure rather sensitively changes with the state of the ionic aggregates. This paper presents IR spectral studies for ethylene−methacrylic acid copolymer (EMAA) neutralized with Co(II) and its complex salts with an organic amine, 1,3-bis(aminomethyl)cyclohexane [1,3-$(NH_2CH_2)_2C_6H_{10}$] (BAC). The structural change near T_i is discussed from IR spectral studies over a wide temperature range, from room temperature to 120 °C.

Previously we reported that the Co(II) salts of EMAA adsorb oxygen molecules whose adsorption sites are in the cobalt(II) carboxylate salts[37] and that the oxygen adsorption may be related to the coordination structure of the Co(II) salts. Moreover, the adsorbed oxygen molecules were found to gradually decompose EMAA ionomers. This work will clarify how the thermal degradation of Co(II) ionomers proceeds with the oxidation, by use of IR spectroscopy and gas chromatography−mass spectrometry (GC−MS). It is pointed out that the oxidation mechanism is connected with the coordination structure of the Co(II) salts.

Experimental Section

Materials. The starting EMAA polymer was from Du Pont-Mitsui Polychemicals Co. Ltd., whose MAA content was 5.4 mol %. The Co(II) salts of EMAA and their complex salts with BAC were prepared via a melt reaction in an extruder at 140−260 °C, as described previously.[17,19] The pellet samples obtained were compression-molded into sheets at about 160 °C and stored at room temperature in a vacuum desiccator for more than 1 month prior to use. We denote the present

† Gifu University.
‡ Du Pont-Mitsui Polychemicals Co. Ltd.
⊗ Abstract published in *Advance ACS Abstracts,* May 1, 1996.

S0024-9297(95)00495-5 CCC: $12.00

ionomer system as EMAA-*x*Co-*y*BAC, where *x* is the degree of neutralization by Co(II) and *y* is the molar equivalent ratio of BAC to COOH group (BAC is a divalent base).

Measurements. Differential scanning calorimetric (DSC) measurements were carried out with a Du Pont DSC-990 calorimeter at a heating/cooling rate of 10 K/min under a dry N_2 flow of ca. 50 mL/min. The specimens were taken from the pellet samples and aged at room temperature for 30 days in a moisture barrier bag before measurements.

IR spectra were measured for ca. 50-μm-thick films with a Perkin-Elmer 1640 FT-IR spectrometer, where 64 scans at a resolution of 4 cm^{-1} were signal-averaged. IR spectra at elevated temperatures were obtained by using a heated cell (S.T. Japan, type 0019-201) and a temperature controller (S.T. Japan, type 0019-200). The following two methods were used for mounting the sample films in the heated cell: (1) The spectra in air were measured by setting the sample film in the heated cell in an open state. (2) The sample film was tightly sandwiched between two KBr windows and then placed in the heated cell. As reported previously,[37] EMAA-0.6Co is gradually oxidized in air at room temperature, and the reaction rate of this oxidation is accelerated when the temperature is raised above ca. 90 °C. Method 2 protected the sample from oxidation during the measurements. Temperatures were monitored by a calibrated Fe constantan thermocouple, which directly touched the sample films in method 1 or was inserted into a hole drilled in the KBr window in method 2. The temperatures were controlled to within ±1 °C.

EMAA-0.6Co is gradually oxidized in air at room temperature and generates decomposition products. Identification of the decomposition products was performed by gas chromatography−mass spectrometry (GC−MS). About 1 g of the sample, which had been stored in air for more than 3 years at room temperature, was heated at 70 °C for 1 h under vacuum, and gaseous decomposition products were collected by use of a GC collecting tube (Shimadzu, TENAX) at −15 °C. The GC collecting tube was then rapidly heated to 200 °C under He gas flow, and the detrapped materials were introduced into a GC−MS spectrometer (JEOL, JMS-DX300). Gas chromatography was obtained by heating a J & W DB-Wax column from 60 to 220 °C at a rate of 4 °C/min under He gas flow, and the mass spectrometer was operated in the electron injection mode with an ionization voltage of 70 kV and an ionization current of 300 μA.

Results and Discussion

Figure 1 shows DSC curves for EMAA-0.6Co and EMAA-0.6Co-0.6BAC, where the first heating curves are for the samples aged at room temperature for 30 days. In the first heating, the curves show two endothermic peaks near 50 and 90 °C, which are assigned to the order−disorder transition of ionic aggregates in our model, as described in the Introduction, and the melting of poly(ethylene) crystallites, respectively, while in the subsequent first cooling process, one exothermic peak is seen around 55 °C, corresponding to the recrystallization of poly(ethylene) chains. In the second heating run started just after the first cooling, the 50 °C peak disappears and only one endothermic peak is observed near 90 °C. However, the 50 °C peak appears and gradually becomes bigger, as the ionomers are stored at room temperature after the second cooling. These thermal hystereses are commonly seen for ethylene ionomers, which we explain by the order−disorder transition model.

Figure 2 shows IR spectra in the region of 1100−1800 cm^{-1} at room temperature for EMAA-*x*Co, and Table 1 lists the peak frequencies for EMAA-*x*Co and EMAA-0.6Co-0.6BAC and their assignments.[2,27−36,38−40] EMAA-*x*Co shows a C═O stretching band of unneutralized carboxylic acid dimers [ν(C═O)] near 1700 cm^{-1} and

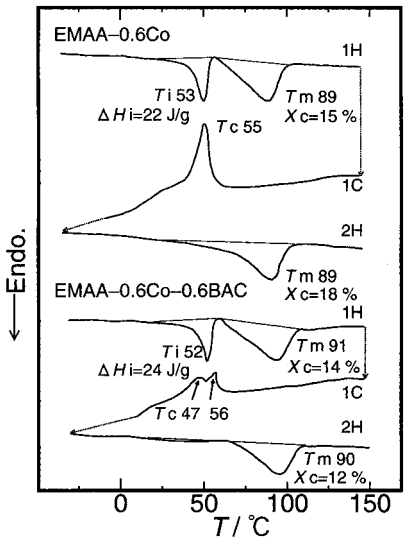

Figure 1. DSC curves for EMAA-0.6Co and EMAA-0.6Co-0.6BAC: 1H, first heating; 1C, first cooling; 2H, second heating measured immediately after the first cooling. T_i, ΔH_i, T_m, T_c, and X_c are transition temperature of order−disorder transition (°C), its enthalpy change, melting point of poly(ethylene) crystallites (°C), their recrystallization temperature (°C) and crystallinity of the poly(ethylene) crystalline region, respectively.

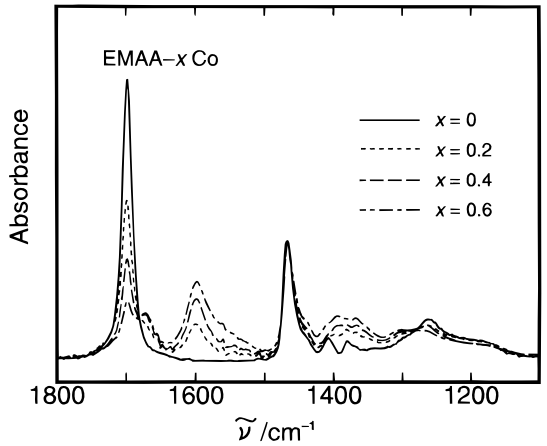

Figure 2. IR spectra in the region of 1100−1800 cm^{-1} for EMAA-*x*Co at room temperature.

asymmetric [$\nu_{as}(COO^-)$] and symmetric COO^- stretching bands [$\nu_s(COO^-)$] near 1600 and 1400 cm^{-1}, respectively. With increasing *x*, the intensity decreases in the ν(C═O) band while it increases in the $\nu_{as}(COO^-)$ and $\nu_s(COO^-)$ bands. Moreover, a new band near 1673 cm^{-1} is seen in EMAA-0.4Co and EMAA-0.6Co. In several metal salts of EMAA, Han and Williams[33,34] found that the ν(C═O) band shifts to lower frequencies with increasing neutralization, and this shift may result from the formation of acid−base complexes between metal cations acting as Lewis acid and unneutralized carboxylic acid groups. According to their assignments, the 1673 cm^{-1} bands might be attributable to the C═O stretching band of hydrogen-bonded COOH dimers whose oxygen atoms would weakly coordinate to Co(II) ions, because the formation of a weak bond between the oxygen atom and the Co(II) ion should lower the electron density of the C═O bond, shifting the C═O band to lower frequencies.

Figure 3 shows the temperature dependence of the IR spectra in the region of 1300−1800 cm^{-1} for EMAA-0.6Co, where the spectra are measured upon heating in the state sealed from air (method 2). The spectrum

Table 1. Observed IR Frequencies (cm^{-1}) of the EMAA-*x*Co-*y*BAC Ionomers

EMAA	EMAA-0.2Co	EMAA-0.4Co	EMAA-0.6Co	EMAA-0.6Co-0.6BAC	assignment
1698	1699	1699	1698	1698	ν(C=O) of hydrogen-bonded $(COOH)_2$
	~1670(sh)	1674	1673		ν(C=O→Co)[a]
	1599	1599	1599	1584 1559[b]	$\nu_{as}(COO^-)$
1467	1467	1467	1467	1467	$\delta_s(CH_2)$
1408	1406(sh)	1405(sh)	~1410		δ(COH)
	1398	1392	1394	1405	$\nu_s(COO^-)$
1382	1382	1382	1383		$\delta_s(CH_3)$
1370(sh)	1368	1368	1368	1369	$\omega(CH_2)$
~1300	1303(sh)	1303(sh)	1302	1307	$\omega(CH_2)$
1262	1264	1264	1266(sh)	1264(sh)	ν(C—O) of hydrogen-bonded $(COOH)_2$
720	720	720	720	720	$\rho(CH_2)$

[a] See text. [b] Overlapping with $\delta_s(NH_3)$; see text. sh, oberved as a shoulder.

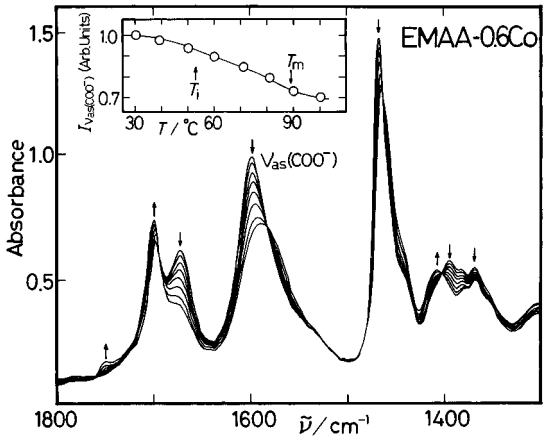

Figure 3. Temperature dependence of IR spectra in the region of 1300−1800 cm^{-1} for EMAA-06Co in the state sealed from air (method 2). Arrows indicate the variation in the IR bands with increasing temperature, where each curve is the spectrum at 30, 39, 50, 60, 71, 81, 90, and 100 °C, respectively. The inset shows the temperature dependence of the peak intensity of the $\nu_{as}(COO^-)$ band.

completely reverted to the original one when the sample was cooled to room temperature after this experiment. The spectra show the characteristic peaks near 1670−1700, 1570−1600, and 1395−1400 cm^{-1}, corresponding to C=O stretching vibration, asymmetric stretching [$\nu_{as}(COO^-)$], and symmetric stretching vibration [$\nu_s(COO^-)$], respectively. The $\nu_{as}(COO^-)$ band locates at 1598 cm^{-1} at room temperature, while as the temperature increases from 30 to 100 °C it gradually becomes broader and shifts to lower frequencies (1570 cm^{-1} at 100 °C), showing an isosbestic point at 1582 cm^{-1}. The existence of the isosbestic point suggests that the Co(II) ions are in at least two different environments, corresponding to two bands at 1598 and ~1570 cm^{-1}, where the latter frequency was determined from the difference spectrum between the spectra at 30 and 100 °C; as the temperature difference increases, the difference spectra decrease in intensity for the 1601 cm^{-1} peak and increase for the 1570 cm^{-1} peak. Therefore, the COO^- ion is considered to be in two states that are in equilibrium with each other, and the state corresponding to the 1570 cm^{-1} band prevails at higher temperatures. The $\nu_s(COO^-)$ band is observed at 1394 cm^{-1} at room temperature and with increasing temperature shifts to 1396 cm^{-1} at 60 °C and 1403 cm^{-1} at 80 °C, showing an isosbestic point at 1401 cm^{-1}.

As the temperature increases, the 1673 cm^{-1} band decreases in the intensity, while the 1698 cm^{-1} band increases, showing an isosbestic point at 1694 cm^{-1}. This result suggests that both 1698 and 1673 cm^{-1} bands originate from the C=O stretching vibrations of hydrogen-bonded COOH dimers and that the two states of dimeric COOH groups, corresponding to the two bands, exist in an equilibrium state with each other. As described already and will be again, we think that the 1673 cm^{-1} band is related to the formation of acid−base complexes between Co(II) ions and dimeric COOH groups. Above 80 °C, another band appears at 1749 cm^{-1}, which is assigned to the C=O stretching band of free, i.e., monomeric, COOH groups. In the inset of Figure 3, the intensity of $\nu_{as}(COO^-)$ is plotted against temperature. The intensity significantly changes with temperature, and we point out that the change largely occurs around 60 °C, corresponding to a T_i of 53 °C in DSC.

Recently, we investigated visible and ESR spectra of EMAA-*x*Co ionomers.[24] At room temperature, in visible spectra, EMAA-0.6Co showed a broad absorption peak centered at 525 nm with a molar extinction coefficient (ϵ) of 21 $mol^{-1}L\ cm^{-1}$, and the color of the sample looked pale pink. As the temperature was raised from room temperature, the band intensity near 575 nm gradually increased above 40 °C, and the value of ϵ at 580 nm reached ~70 at 130 °C, at which point the sample looked brown. The 525-nm band was attributed to the $^4T_{1g}(F)\rightarrow{}^4T_{1g}(P)$ transition of Co(II) ions in an octahedral coordination field and showed a very small value of ϵ due to the Laporte (parity)-forbidden nature of this transition. The 575-nm band was assigned to the $^4A_2(F)\rightarrow{}^4T_1(P)$ transition of tetrahedrally coordinated Co(II) ions, where the Laporte forbiddance is broken down. These results indicate that the environment of Co(II) ions in EMAA-0.6Co gradually changes from octahedral to tetrahedral coordination above T_i (53 °C). Strictly speaking, only a small portion of the octahedrally coordinated Co(II) ions is transformed into those of tetrahedral coordination above T_i, because the ϵ value is usually 100−1000 for the $^4A_2(F)\rightarrow{}^4T_1(P)$ transition but was ~70 even at 130 °C for EMAA-0.6Co.[41] The ESR spectral data supported this change in the coordination structure with temperature.

By referring to these visible spectral data, the characteristic IR spectral changes with temperature can be well explained by the transformation from octahedral to tetrahedral coordination in the Co(II) salts. In the $\nu_{as}(COO^-)$ band, the 1598 cm^{-1} peak at room temperature may originate from an octahedral coordination structure. When the temperature increases, the octahedral coordination partially transforms into a tetrahedral coordination, resulting in the appearance of and increase in the 1570 cm^{-1} peak. This picture is also observed for the 1673 cm^{-1} band. From the law of electric neutrality, two COO^- groups coordinate to one Co(II) ion as a bidentate ligand. In octahedral coordina-

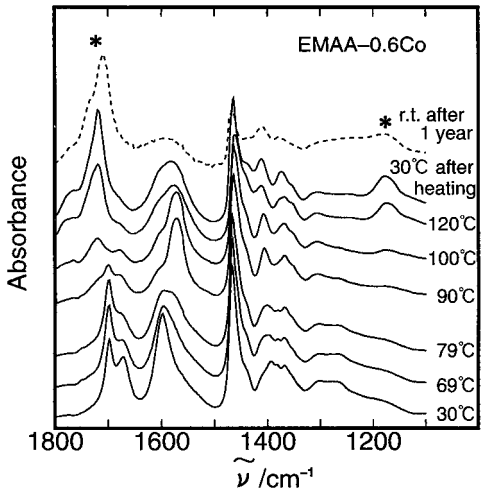

Figure 4. Temperature dependence of IR spectra in the region of 1100−1800 cm^{-1} for EMAA-0.6Co measured in air (method 1). The dashed line shows the spectrum for EMAA-0.6Co aged in air for more than 1 year at room temperature. Two asterisks denote the new absorption bands appearing during aging air.

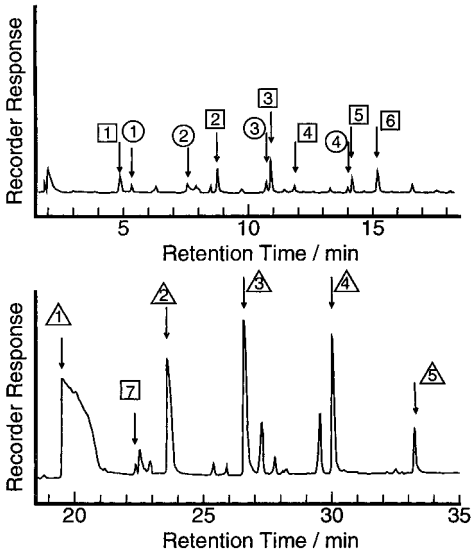

Figure 5. GC−MS chromatogram for oxidation−decomposition products from EMAA-0.6Co aged in air for more than 3 years at room temperature. Peak numbers refer to the compounds listed in Table 2. Circles, squares, and triangles denote alcohols, ketones, and alkanecarboxylic acids, respectively.

tion, the $(COO)_2Co(II)$ unit needs two more oxygens, which should be supplied from the hydrogen-bonded carbonyl groups. As the result, the coordinated carbonyl groups exhibit the 1673 cm^{-1} band. Consequently, the 1673 cm^{-1} band may be attributable to the C=O stretching band of hydrogen-bonded COOH dimers whose oxygen atoms weakly coordinate to Co(II) ions. When EMAA-0.6Co is heated, the octahedrally coordinated Co(II) ions are partially transformed into tetrahedrally coordinated ones. This transformation decreases the number of hydrogen-bonded carbonyl groups coordinating to the Co(II) ion, leading to decreasing intensity of the 1673 cm^{-1} band. It should be emphasized that the present IR results seem to support the presence of the order−disorder transition in ionic aggregate regions at T_i, because the change in coordination environments with temperature takes place around T_i in spite of a broad change.

Figure 4 shows the temperature dependence of the IR spectra measured in air (method 1) in the region of 1100−1800 cm^{-1} of EMAA-0.6Co. The spectral pattern below 80 °C is almost the same as that measured in the state sealed from air (method 2); with increasing temperature, the $\nu_{as}(COO^-)$ band at 1598 cm^{-1} decreases, accompanied by the appearance of a band near 1570 cm^{-1}, while the C=O stretching vibration band near 1673 cm^{-1} decreases and the band near 1698 cm^{-1} increases. However, when the temperature is higher than 80 °C, the $\nu_{as}(COO^-)$ band gradually shifts to lower frequencies (e.g., 1596 cm^{-1} at 79 °C and 1571 cm^{-1} at 90 °C) and becomes more intense, and then it becomes a very broad peak near 1576 cm^{-1} above 100 °C. On the other hand, two new peaks at 1720 and 1180 cm^{-1}, marked with an asterisk in Figure 4, appear and develop above 80 °C. It is noted that even at 30 °C these two peaks remain as intense bands for the sample cooled after heating at 120 °C once, as well as for the sample aged in air for about 1 year at room temperature. In previous visible and ESR spectral studies,[37] we found that EMAA-0.6Co is gradually oxidized in air at room temperature, and the oxidation reaction is promoted with increasing temperature. Therefore, the 1720 and 1180 cm^{-1} bands are concluded to come from oxidation in air.

The GC−MS chromatographic measurements were carried out to detect what products are generated from EMAA-*x*Co systems by oxidation−degradation. The data are shown in Figure 5 and Table 2 for EMAA-0.6Co aged in air for more than 3 years. Several alcohols, 2- or 3-ketones, and alkanecarboxylic acids are found as the decomposition products. The elution order of alcohols is associated with their boiling points, and a similar trend is also observed for both ketone and acid series. The presence of valeric acid and caproic acid means a breaking of backbone chains. The 1720 and 1180 cm^{-1} peaks may be related to these decomposition products, and therefore, we can assign the 1720 cm^{-1} peak to the carbonyl stretching bands of ketones and the 1180 cm^{-1} peak to the C−C(O)−C stretching or bending of ketones, respectively.[40]

Figure 6 shows the temperature dependence of the IR spectra in the region of 1100−1800 cm^{-1} for EMAA-0.6Co-0.6BAC. The spectrum of EMAA-0.6Co-0.6BAC is different from that of EMAA-0.6Co (Figure 2) as follows: (1) the $\nu_{as}(COO^-)$ absorption, which is observed as a peak at 1599 cm^{-1} for EMAA-0.6Co, splits into two peaks at 1584 and 1559 cm^{-1}; (2) the $\nu_s(COO^-)$ band shifts to 1405 cm^{-1}, compared with 1394 cm^{-1} for EMAA-0.6Co; and (3) the ν(C=O) band near 1698 cm^{-1}, attributable to the C=O stretching vibrations of hydrogen-bonded COOH dimers, largely diminishes. From the previous visible spectral studies,[24] we found that most of the Co(II) ions form a tetrahedral coordination structure in EMAA-0.6Co-0.6BAC at room temperature, in contrast with the octahedral coordination in the EMAA-*x*Co system. The changes in the 1 and 2 points may correspond to the change from octahedral to tetrahedral coordination of Co(II) ions with the addition of BAC. The 3 point, on the other hand, indicates that a part of the BAC added reacts with COOH groups to form ammonium salts such as $COO^-NH_3^+$. In fact, EMAA-0.4BAC, where 40% of the COOH groups in EMAA are neutralized with BAC, exhibits an asymmetric NH_3^+ bending band at 1636 cm^{-1} and a symmetric NH_3^+ band at 1521 cm^{-1},[40] which in EMAA-0.6Co-0.6BAC appear to overlap with the 1584 cm^{-1}

Table 2. List of Oxidation−Decomposition Products Detected by GC−MS for Fully Oxidized EMAA-0.6Co[a]

alcohols	ketones	carboxylic acids
1. CH_3CH_2OH MW 46, bp 78 °C	1. $CH_3CH_2C(O)CH_3$ MW 72. bp 80 °C	1. CH_3COOH MW 60, bp 118 °C
2. $CH_3(CH_2)_2OH$ MW 60, bp 97 °C	2. $CH_3(CH_2)_3C(O)CH_3$ MW 100, bp 128 °C	2. CH_3CH_2COOH MW 74, bp 141 °C
3. $CH_3(CH_2)_3OH$ MW 74, bp 118 °C	3. $CH_3(CH_2)_3C(O)CH_2CH_3$ MW 114, bp 144 °C	3. $CH_3(CH_2)_2COOH$ MW 88, bp 162 °C
4. $CH_3(CH_2)_4OH$ MW 88, bp 138 °C	4. $CH_3(CH_2)_4C(O)CH_3$ MW 114, bp 144 °C	4. $CH_3(CH_2)_3COOH$ MW 102, bp 186−187 °C
	5. $CH_3(CH_2)_4C(O)CH_2CH_3$ MW 128, bp 169 °C	5. $CH_3(CH_2)_4COOH$ MW 117, bp 205 °C
	6. $CH_3(CH_2)_5C(O)CH_3$ MW 128, bp 174 °C	
	7. $CH_3(CH_2)_7C(O)CH_3$ MW 156, bp ~215 °C	

[a] MW, molecular weight; bp, boiling point.

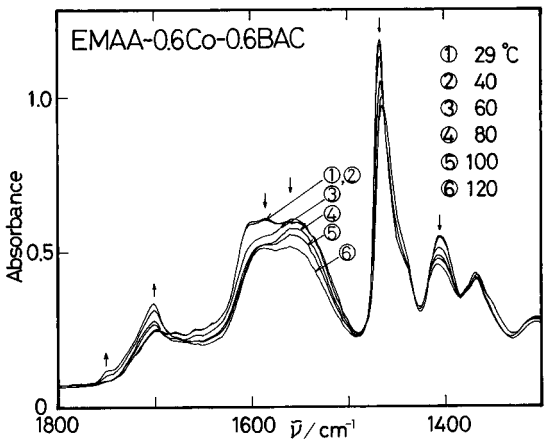

Figure 6. Temperature dependence of IR spectra in the region of 1300−1800 cm^{-1} for EMAA-0.6Co−0.6BAC measured in air (method 1). Arrows indicate the variation in the IR bands with increasing temperature.

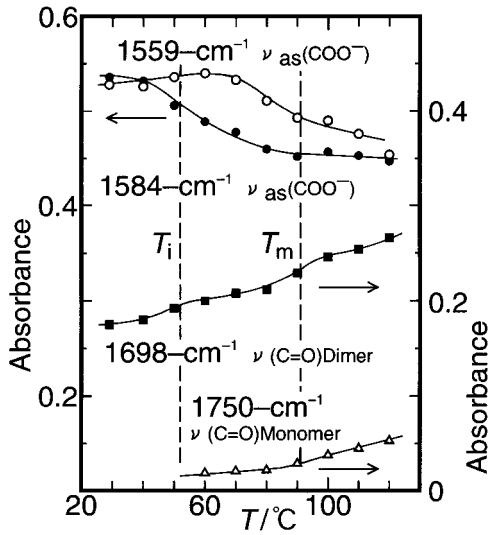

Figure 7. Plots of the peak intensities vs temperature for two $\nu_{as}(COO^-)$ bands at 1584 (●) and 1559 cm^{-1} (○) and two ν(C═O) bands at 1750 (△) and 1698 cm^{-1} (■).

band and 1559 cm^{-1} band, respectively, but certainly exist.

In contrast with EMAA-0.6Co, the IR spectrum of EMAA-0.6Co-0.6BAC was reversible with temperature even when the temperature was raised above T_m in air. Therefore, BAC acts as an inhibitor for the oxidation, and so the addition of BAC significantly enhances the thermal stability of the EMAA ionomers containing Co(II) ions, which may result from the formation of the tetrahedrally coordinated Co(II) complexes. In EMAA-0.6Co, uncoordinated sites would somewhat exist in octahedrally coordinated (i.e., hexacoordinated) Co(II) ions, because restricted mobility of the coordinating atoms (i.e., oxygen atoms of COO^- and COOH) and steric hindrance around Co(II) ions in polymer would sometimes prohibit the completion of a hexacoordinated structure. The uncoordinated sites can act as the adsorption sites for oxygen molecules. A similar procedure has been deduced in understanding the oxygen-adsorption behavior of model hemoglobins.[42] The completion of four coordinations, on the contrary, can be more easily achieved in EMAA-0.6Co-0.6BAC and, of course, afford no adsorption site for oxygen molecules.

In Figure 6, two $\nu_{as}(COO^-)$ bands at 1584 and 1559 cm^{-1} and two ν(C═O) bands at 1750 and 1698 cm^{-1} significantly change with temperature. Their peak absorbances are plotted in Figure 7 as a function of temperature. The intensities of two $\nu_{as}(COO^-)$ bands are almost unchanged with temperature below 40 °C. As the temperature increases more, however, the intensity of the 1584 cm^{-1} band begins to decrease around T_i (52 °C), and the decrease ceases above ~T_m (91 °C). On the other hand, the intensity of the 1559 cm^{-1} band is almost unchanged until 70 °C above the T_i and begins to decrease from about 80 °C just below T_m. The decrease in intensity of the 1584 cm^{-1} band can be ascribed to some change in the environment of the Co(II) ions, while that of the 1559 cm^{-1} band may be due to a combination effect of some change in the environment of the Co(II) ions (other than those corresponding to the 1584 cm^{-1} band) and a weak dissociation of $COO^-NH_3^+$ to COOH and NH_2. Moreover, the intensities of two ν(C═O) bands at 1698 and 1750 cm^{-1}, corresponding to the dimeric and monomeric carbonyl stretching vibrations, respectively, gradually increase with increasing temperature, and these increases become rather prominent above 80 °C. This result suggests a gradual dissociation of $COO^-NH_3^+$ with temperature. Finally, the temperature dependence of the spectra is reversible, as already described, and, in particular, the 1559 cm^{-1} band completely reverted to the original one after the sample was cooled to room temperature. This result excludes any possibility of sample decomposition. Consequently, spectral changes begin to occur near the T_i of EMAA-0.6Co-0.6BAC and certainly reflect some structural change in the ionic aggregate regions of EMAA-0.6Co-0.6BAC. These observations are regarded as evidence for our order−disorder transition model of ionic aggregate regions.

The transition at T_i in DSC is irreversible with temperature, as shown in Figure 1, whereas the IR spectral change near T_i is reversible with temperature. By assuming the order−disorder transition model,[11] when ionomers are cooled from a temperature above T_i, the reorganization of disordered ionic aggregate regions requires a relaxation time of about 30 days at room temperature, and this relaxational change proceeds through two steps, a faster process (F process) and a slower process (S process): A reordering of the first coordination shell around ions may occur almost *adiabatically* (F process), resulting in an unequilibrium between the first coordination shell and its surrounding portion, where the latter portion includes the neighboring ions and the short segments of backbone chains attached to the ionic groups. Then, the preceding two portions may gradually relax, as a whole, to a final equilibrium state with a longer relaxation time (S process). For EMAA-0.6Co-0.6BAC, the relaxation times (τ) for these two processes were calculated according to the method described in a previous paper.[11] The value of τ for the F process was estimated to be 25 min at 55 °C and 0.87 day at 25 °C, and the value of τ for the S process was 1.1 h at 55 °C and 19 days at 25 °C. DSC may mainly detect the S process. The ν(C=O) and $\nu_{as}(COO^-)$ bands in the IR spectra, on the other hand, would be sensitive to a change in the first coordination shell, which corresponds to the F process. The F process is essentially reversible with temperature, which seems to be consistent with the reversibility of the IR spectrum with temperature. Therefore, the changes in the IR spectra near T_i may originate in the order−disorder transition model of ionic aggregate regions and do not contradict the thermal hysteresis of the T_i peak on DSC. Finally, it should be noted that a trigger of the transition at T_i may be a melting of the ordered segments of ethylene chains adjacent to the cobalt(II) carboxylate groups, as pointed out in our previous paper.[14] This may be a cause of the rather broad change in the $\nu_{as}(COO^-)$ bands centered at T_i.

Conclusions

In this work, the coordination structure and its change with temperature of Co(II) ions in EMAA-Co and EMAA-Co-BAC systems were investigated by IR spectroscopic measurements. The IR spectrum of EMAA-0.6Co at room temperature showed a shoulder band at 1673 cm^{-1}, which demonstrated that the two carbonyl oxygens of $(COOH)_2$ dimers weakly coordinate to Co(II) ions to form hexacoordination (octahedral coordination) of oxygens. When the samples were heated in the absence of air, the intensity of the 1673 cm^{-1} band decreased, suggesting breakage of the weak coordination bond and a progressive transformation toward tetracoordination. In air, on the other hand, the spectral change with temperature was irreversible, reflecting the presence of oxidation−degradation. The decomposition products were determined by GC−MS measurements. The main components were alcohol, ketone, and alkanecarboxylic acid derivatives, and the generation of acid derivatives containing five or six carbon atoms suggests a breaking of backbone chains. In contrast to EMAA-0.6Co, the spectral change with temperature was found to be reversible in EMAA-0.6Co-BAC, even when the sample was heated in air above T_m. This observation suggests that the organic amine (BAC) acts as a stabilizer. It is pointed out that the tetracoordination around Co(II) ions in EMAA-0.6Co-0.6BAC is responsible for the improved stability against oxidation−degradation, and in EMAA-0.6Co uncoordinated sites of hexacoordinated Co(II) ions may act as adsorption sites for oxygen molecules. Thus, the coordination structure of the Co(II) ions provides a profound influence on the stability against oxidation−degradation. For both EMAA-0.6Co and EMAA-0.6Co-0.6BAC, it was found that the $\nu_{as}(COO^-)$ band, which is sensitive to changes in coordination environment around Co(II) ions, significantly changes near an order−disorder transition temperature, T_i, of ionic aggregate regions. This result, together with the previous visible spectral and ESR results, supports the order−disorder transition model of ionic aggregate regions proposed by our group.

Acknowledgment. We thank Mr. Yukiyoshi Sakaida for his kind help. We also thank Prof. Kenji Tadano of Gifu College of Medical Technology, Prof. Jun Yamauchi of Kyoto University, and Mr. Yoshikazu Kutsuwa of Du Pont-Mitsui Polychemicals Co. Ltd. for valuable suggestions and discussions. This work was partly supported by Grants-in-Aid for Scientific Research (Nos. 05555254 and 07650797) from the Ministry of Education, Science, and Culture of Japan.

References and Notes

(1) Eisenberg, A. *Macromolecules* **1970**, *3*, 147.
(2) Holliday, L., Ed. *Ionic Polymers*; Applied Science: London, 1975.
(3) Eisenberg, A.; King, M. *Ion-Containing Polymers, Physical Properties and Structure, Polymer Physics*; Academic Press: New York, 1977; Vol. 2.
(4) Pineri, M., Eisenberg, A., Eds. *Structure and Properties of Ionomers*; NATO ASI Series C, Mathematical and Physical Sciences; D. Reidel Co.: Dordrecht, The Netherlands, 1987; Vol. 198.
(5) Utracki, L. A., Weiss, R. A., Eds. *Multiphase Polymers: Blends and Ionomers*; ACS Symposium Series 395; American Chemical Society: Washington, DC, 1989.
(6) MacKnight, W. J.; Taggart, W. P.; Stein, R. S. *J. Polym. Sci., Symp.* **1974**, *45*, 113.
(7) Moudden, A.; Levelut, A. M.; Pineri, M. *J. Polym. Sci., Polym. Phys. Ed.* **1977**, *15*, 1707.
(8) Yarusso, D. J.; Cooper, S. L. *Macromolecules* **1983**, *16*, 1871.
(9) Eisenberg, A.; Hird, B.; Moore, R. B. *Macromolecules* **1990**, *23*, 4098.
(10) Tadano, K.; Hirasawa. E.; Yamamoto, Y.; Yamamoto, H.; Yano, S. *Jpn. J. Appl. Phys.* **1987**, *26*, L1440.
(11) Tadano, K.; Hirasawa, E.; Yamamoto, H.; Yano, S. *Macromolecules* **1989**, *22*, 226.
(12) Hirasawa, E.; Yamamoto, Y.; Tadano, K.; Yano, S. *Macromolecules* **1989**, *22*, 2776.
(13) Kutsumizu, S.; Nagao, N.; Tadano, K.; Tachino, H.; Hirasawa, E.; Yano, S. *Macromolecules* **1992**, *25*, 6829.
(14) Yano, S.; Tadano, K.; Nagao, N.; Kutsumizu, S.; Tachino, H.; Hirasawa, E. *Macromolecules* **1992**, *25*, 7168.
(15) Yano, S.; Yamamoto, H.; Tadano, K.; Yamamoto, Y.; Hirasawa, E. *Polymer* **1987**, *28*, 1965.
(16) Yano, S.; Nagao, N.; Hattori, M.; Hirasawa, E.; Tadano, K. *Macromolecules* **1992**, *25*, 368.
(17) Hirasawa, E.; Yamamoto, Y.; Tadano, K.; Yano, S. *J. Appl. Polym. Sci.* **1991**, *42*, 351.
(18) Hirasawa, E.; Hamazaki, H.; Tadano, K.; Yano, S. *J. Appl. Polym. Sci.* **1991**, *42*, 621.
(19) Hirasawa, E.; Tadano, K.; Yano, S. *J. Polym. Sci., Polym. Phys. Ed.* **1991**, *29*, 753.
(20) Tachino, H.; Hara, H.; Hirasawa, E.; Kutsumizu, S.; Tadano, K.; Yano, S. *Macromolecules* **1993**, *26*, 752.
(21) Kutsumizu, S.; Hashimoto, Y.; Yano, S.; Hirasawa, E. *Macromolecules* **1991**, *24*, 2629.
(22) Tsunashima, K.; Nishioji, H.; Hirasawa, E.; Yano, S. *Polymer* **1992**, *33*, 1809.
(23) Tsunashima, K.; Kutsumizu, S.; Hirasawa, E.; Yano, S. *Macromolecules* **1991**, *24*, 5910.
(24) Yano, S.; Tadano, K.; Hirasawa, E.; Yamauchi, J. *Polym. J.* **1991**, *23*, 969.
(25) Takei, M.; Tsujita, Y.; Shimada, S.; Ichihara, H.; Enokida, M.; Takizawa, A.; Kinoshita, T. *J. Polym. Sci., Polym. Phys. Ed.* **1988**, *26*, 997.

(26) Yamauchi, J.; Narita, H.; Kutsumizu, S.; Yano, S. *Macromol. Chem. Phys.* **1995**, *196*, 3919.
(27) Coleman, M. M.; Painter, P. C. *J. Macromol. Sci., Rev. Macromol. Chem.* **1977/1978**, *C16*, 197.
(28) Andreeva, E. D.; Nikitin, V. N.; Boyartchuk, Y. M. *Macromolecules* **1976**, *9*, 238.
(29) Painter, P. C.; Brozoski, B. A.; Coleman, M. M. *J. Polym. Sci., Polym. Phys. Ed.* **1982**, *20*, 1069.
(30) Brozoski, B. A.; Coleman, M. M.; Painter, P. C. *J. Polym. Sci., Polym. Phys. Ed.* **1983**, *21*, 301.
(31) Brozoski, B. A.; Coleman, M. M.; Painter, P. C. *Macromolecules* **1984**, *17*, 230.
(32) Brozoski, B. A.; Painter, P. C.; Coleman, M. M. *Macromolecules* **1984**, *17*, 1591.
(33) Han, K.; Williams, H. L. *J. Appl. Polym. Sci.* **1989**, *38*, 73.
(34) Han, K.; Williams, H. L. *J. Appl. Polym. Sci.* **1990**, *42*, 1845.
(35) Coleman, M. M.; Lee, J. Y.; Painter, P. C. *Macromolecules* **1990**, *23*, 2339.
(36) Ishioka, T. *Polym. J.* **1993**, *25*, 1147.
(37) Yano, S.; Tadano, K.; Hirasawa, E.; Yamauchi, J. *Macromolecules* **1990**, *23*, 4872.
(38) Synder, R. G. *J. Chem. Phys.* **1967**, *47*, 1316.
(39) Edwards, D. A.; Hayward, R. N. *Can. J. Chem.* **1968**, *46*, 3443.
(40) Silverstein, R. M.; Bassler, G. C.; Morrill, T. C. *Spectroscopic Identification of Organic Compounds*; John Wiley & Sons: New York, 1981.
(41) It may be a better to say that a *distortion* in coordination symmetry around Co(II) ions begin to occur near T_i.
(42) For example, Collman, J. P.; Gagne, R. R.; Read, C. A.; Halbert, T. R.; Lang, G.; Robinson, W. T. *J. Am. Chem. Soc.* **1975**, *97*, 1427.

MA950495Q